

## Supplementary Materials for Eukaryotic G Protein Signaling Evolved to Require G Protein–Coupled Receptors for Activation

William Bradford, Adam Buckholz, John Morton, Collin Price, Alan M. Jones,\*  
Daisuke Urano

\*Corresponding author. E-mail: alan\_jones@unc.edu

Published 21 May 2013, *Sci. Signal.* **6**, ra37 (2013)  
DOI: 10.1126/scisignal.2003768

### The PDF file includes:

Fig. S1. Genes encoding heterotrimeric G protein components found in eukaryotic genomes.

Fig. S2. Phylogeny of unikonta GPCRs.

Fig. S3. Minimum spanning network for unikonta GPCRs.

Fig. S4. ML trees of the 7TM-RGS proteins show the distinct origin of 7TM-RGS proteins.

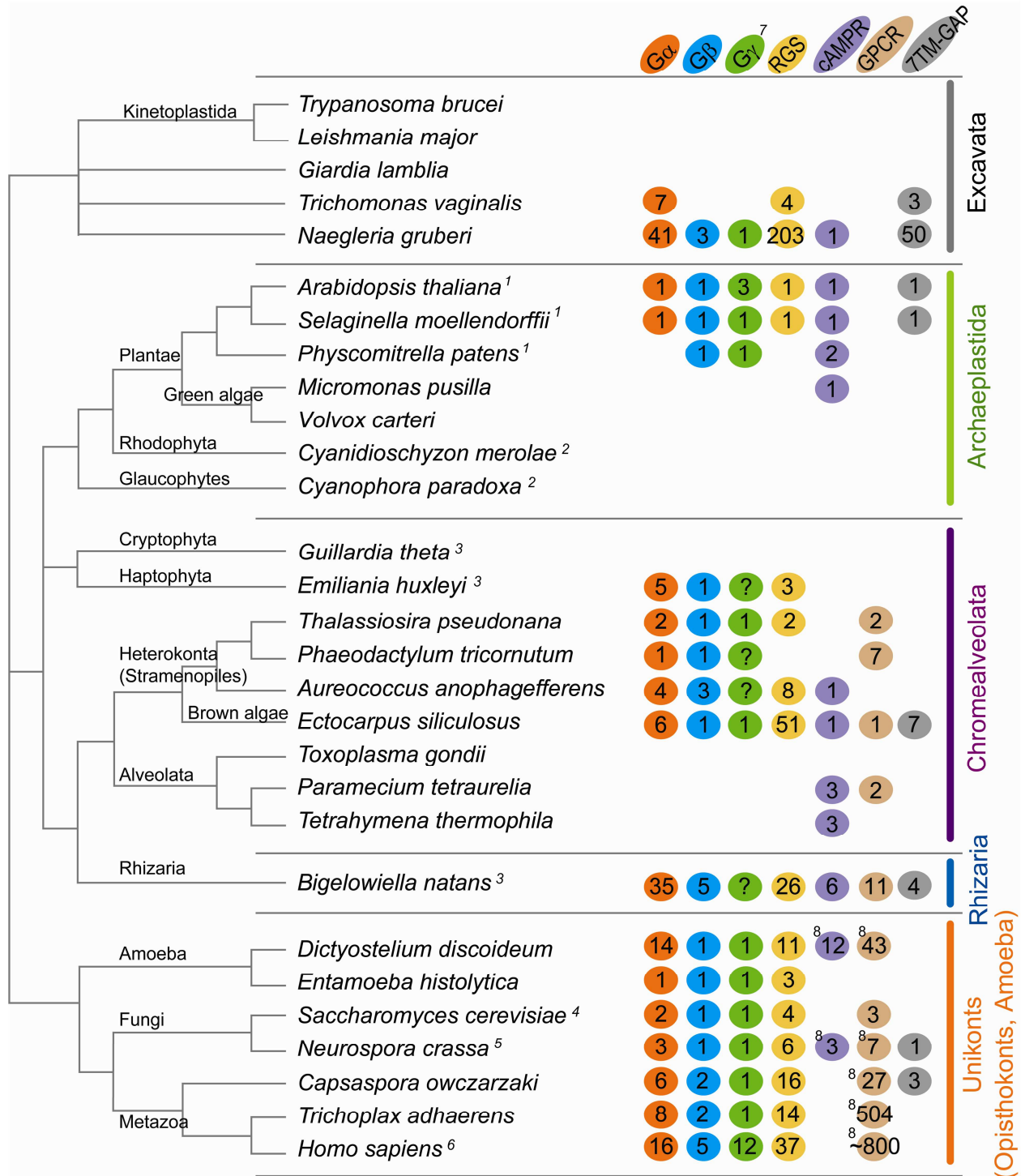
Fig. S5. Intrinsic fluorescence measurements of the nucleotide exchange and hydrolysis activities of G $\alpha$  proteins support the radionucleotide assay–based measurements.

Fig. S6. Identity among *T. vaginalis* G protein components.

Fig. S7. Multiple sequence alignment of G $\alpha$  subunits showing conserved residues.

Table S1. Accession numbers of genes encoding G proteins, RGS proteins, and GPCRs.

References (43–47)



**Fig. S1.** Genes encoding heterotrimeric G protein components found in eukaryotic genomes. The numbers of homologous genes encoding G $\alpha$ , G $\beta$ , G $\gamma$ , RGS, *D. discoideum* cAMP receptor (cAMPR), Opisthokonta GPCRs, and 7TM-RGS proteins. The homologous genes for G $\alpha$  (SM00275), G $\gamma$  (SM00224), RGS (SM00315), cAMP receptor (PF05462), or Opisthokonta GPCRs (PF00001 for the rhodopsin family; PF00002 for the secretin receptor family; PF00003 for the metabolic glutamate receptor family; PF01534 for the Frizzled family; PF02116 for the

yeast STE2 family; and PF11710 for the *Schizosaccharomyces pombe* Git3 family) were collected from the NCBI CDD (<http://www.ncbi.nlm.nih.gov/Structure/cdd/cdd.shtml>) or the JGI (<http://genome.jgi.doe.gov/>). Genes from *Cyanidioschyzon merolae* and *Cyanophora paradoxa* were collected with an HMM-based search engine on the HMMER website (<http://hmmer.janelia.org/>) because their proteome datasets were not available on the NCBI or JGI databases. The genes encoding G $\beta$  and G $\gamma$  were searched for with the HMM-based search engine or on the proteome dataset of individual genomes. Footnotes: [1] The numbers of genes encoding plant G $\alpha$ , G $\beta$ , G $\gamma$ , and RGS proteins were determined from the literature (6). Land plants have canonical and noncanonical G $\alpha$  subunits. The numbers of G $\alpha$ -encoding genes indicated do not include genes encoding noncanonical G $\alpha$  subunits. [2] The proteome datasets were downloaded from the individual genome websites. [3] The genes of these species are from JGI. [4] Genes encoding G proteins and RGS proteins in *S. cerevisiae* are as previously reported (43). [5] *N. crassa* genes encoding G $\alpha$ , G $\beta$ , G $\gamma$ , cAMP receptors, and GPCRs are as previously reviewed (44). [6] Genes encoding human G proteins are as previously reviewed (46). [7] Metazoa have a G $\gamma$ -like (GGL) domain in RGS6 family proteins. The numbers of metazoan G $\gamma$ -encoding genes do not include those containing GGL domains. [8] The unikonta GPCRs were described previously (17, 31, 44, 45). The accession numbers of the genes encoding G proteins and RGS proteins are shown in table S1.

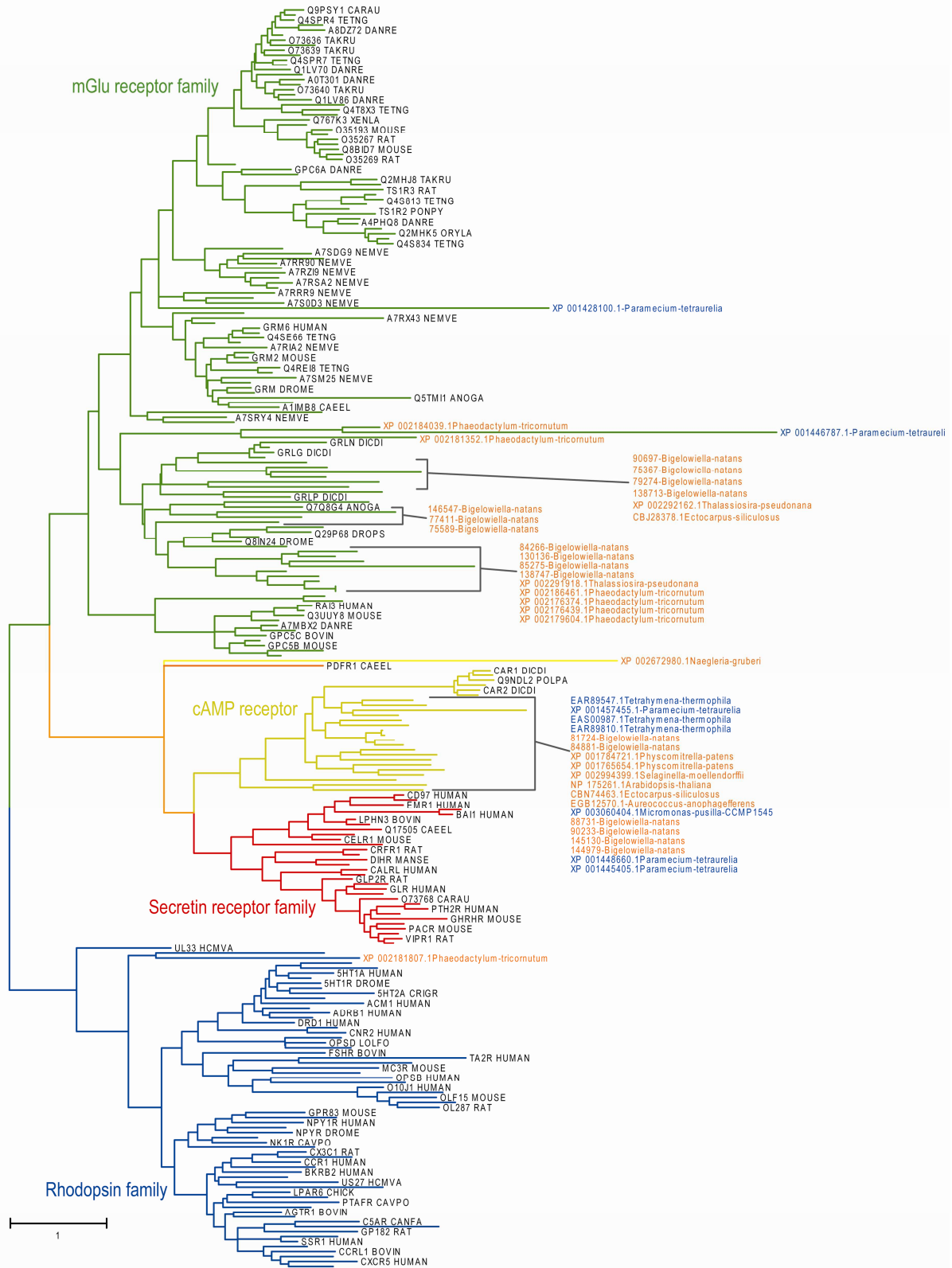


**Fig. S2.** Phylogeny of unikonta GPCRs. The seed protein sequences based on a protein model of GPCRs and bacteriorhodopsin were downloaded from the Pfam26.0 database (rhodopsin family:

PF00001; secretin family: PF00002; metabolic glutamate receptor family: PF00003; cAMP receptor family: PF05462; and bacteriorhodopsin: PF01036). The GPCRs found in bikonts were collected from the NCBI CDD or the JGI protein databases. The sequences were aligned with Clustal W implemented in MEGA5.0 (<http://www.megasoftware.net/>). The ML tree is shown with branches colored in green (Rhodopsin family), yellow (cAMP receptor family), red (secretin receptor family), or blue (Rhodopsin family).

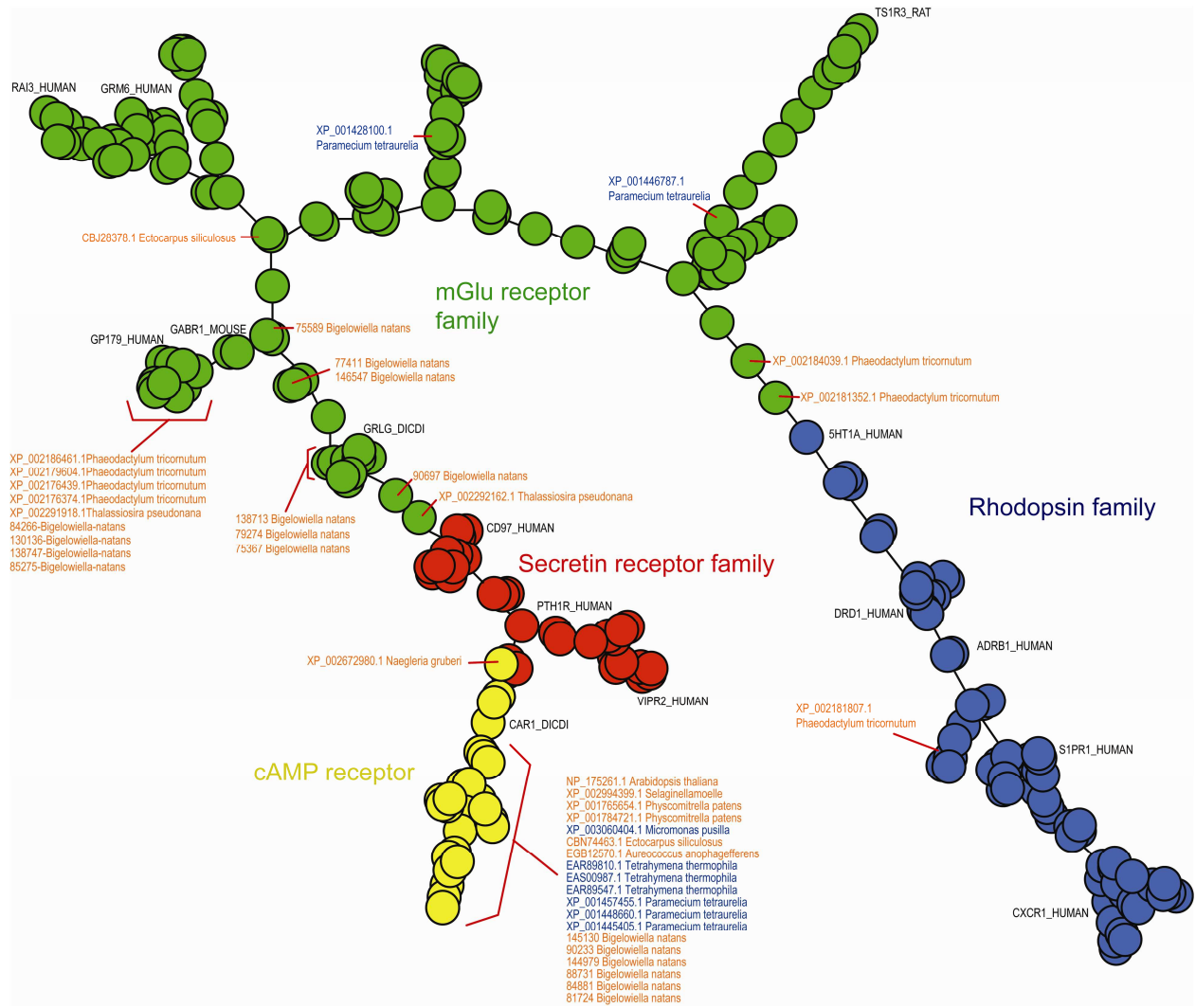


**Fig. S3.** Minimum spanning network for unikonta GPCRs. The protein sequences for GPCRs were prepared as described in fig. S2. The distance between each pair of GPCR sequences was calculated with the ML method implemented in Splitstree 4.0 (41), and the network was constructed with the minimum-spanning network (MSN) algorithm. Color codes of the nodes are as follows: blue: Rhodopsin family; green: metabolic glutamate receptor family; red: secretin receptor family; and yellow: cAMP receptor family. Bikonta GPCRs are shown with their accession number and the species name. Representative GPCRs are shown with their Pfam identifiers.

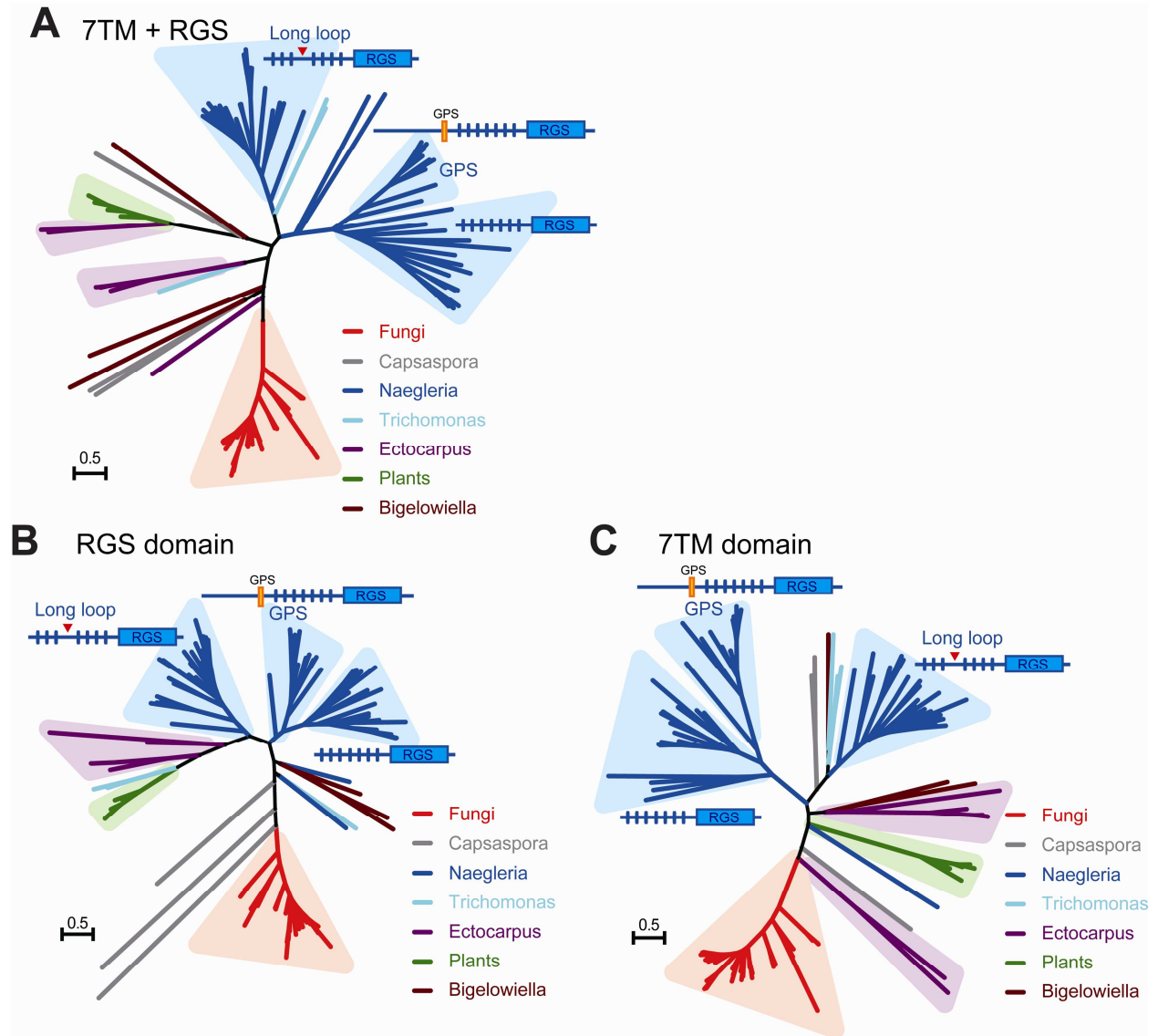


**Fig. S4.** ML trees of the 7TM-RGS proteins show the distinct origin of 7TM-RGS proteins. **(A)** Unrooted tree of the 7TM-RGS sequences. Three types of domain architectures found in *N. gruberi* 7TM-RGS proteins are shown beside the branches. **(B and C)** Unrooted trees of the RGS and the 7TM domains of 7TM-RGS proteins. Note that *Naegleria* has three groups for the 7TM-RGS proteins. Group 1 members have no sequential characteristics, group 2 members have a GPS (GPCR proteolytic site) and a long N-terminal extension, similar to a structure found in mammalian adhesion GPCRs, and group 3 members have a long insertion in the third loop of the 7TM domain. The 7TM domain of group 3 members is unrelated in sequence to those of groups 1 and 2. The RGS domains of plants and *Ectocarpus* are evolutionary close to those of *Trichomonas* and *Naegleria* group 3 members, whereas their 7TM domains are distinct from each other and from those of *Naegleria* and *Trichomonas*. The phylogenetic distribution of bikonta 7TM-RGS proteins indicates that fusion events of the two domains occurred individually in some evolutionary clades.

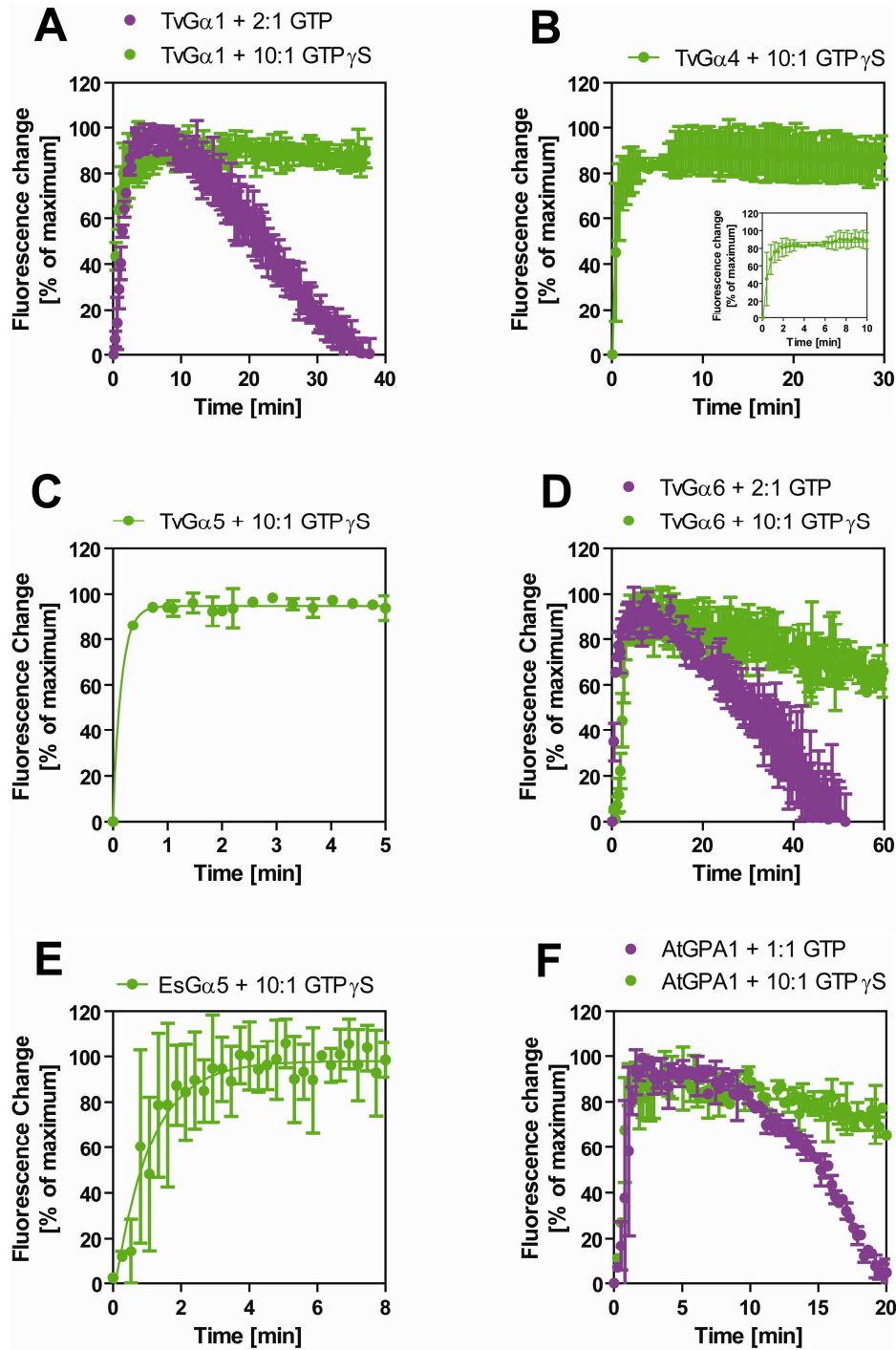


**Fig. S5.** Intrinsic fluorescence measurements of the nucleotide exchange and hydrolysis activities of G $\alpha$  proteins support the radionucleotide assay-based measurements. (A to E) The intrinsic tryptophan fluorescence of 500 nM G $\alpha$  was measured with GTP as indicated or with 5  $\mu$ M GTP $\gamma$ S. Note that TvG $\alpha$ 1 and TvG $\alpha$ 6, which exhibited fast intrinsic nucleotide exchange and slow intrinsic GTP hydrolysis activities, displayed plateaued fluorescence in the presence of hydrolyzable GTP followed by a decrease in fluorescence as the GTP was hydrolyzed (A and D). TvG $\alpha$ 4 and TvG $\alpha$ 5 exhibited rapid exchange in the presence of GTP $\gamma$ S (B and C), further supporting their fast exchange properties. (E) EsG $\alpha$ 5 showed fast exchange in the presence of GTP $\gamma$ S. (F) Nucleotide exchange and hydrolysis behaviors of AtGPA1, a known self-activator, are provided for comparison purposes. Data shown are means  $\pm$  SD of two or three independent experiments.



**A**

<b>Designation</b>	<b>Accession Number</b>
TvGα1	XP_001322334
TvGα2	XP_001330268
TvGα3	XP_001580284
TvGα4	XP_001304281
TvGα5	XP_001325781
TvGα6	XP_001324344
TvRGS1 (5TM)	XP_001311154
TvRGS2 (7TM)	XP_001583271
TvRGS3 (7TM)	XP_001326285
TvRGS4 (7TM)	XP_001320387

**B**

	<b>TvGα1</b>	<b>TvGα2</b>	<b>TvGα3</b>	<b>TvGα4</b>	<b>TvGα5</b>	<b>TvGα6</b>	<b>AtGPA1</b>	<b>HsGai1</b>
<b>TvGα1</b>	X	44%	35%	43%	33%	32%	33%	32%
<b>TvGα2</b>	44%	X	33%	35%	32%	32%	29%	31%
<b>TvGα3</b>	35%	33%	X	31%	49%	40%	30%	31%
<b>TvGα4</b>	43%	35%	31%	X	32%	33%	28%	32%
<b>TvGα5</b>	33%	32%	49%	32%	X	36%	26%	29%
<b>TvGα6</b>	32%	32%	40%	33%	36%	X	28%	29%
<b>AtGPA1</b>	33%	29%	30%	28%	26%	28%	X	37%
<b>HsGai1</b>	32%	31%	31%	32%	29%	29%	37%	X

**Fig. S6.** Identity among *T. vaginalis* G protein components. *T. vaginalis* Gα proteins differ substantially from one another at the primary sequence level. (A) Gene accession numbers of *T. vaginalis* G protein components. (B) Sequence identity among TvGα proteins, *Arabidopsis* GPA1, and human Gα<sub>i1</sub> was determined by the protein BLAST program. Sequence identities of >40% are highlighted in green. The 3D structure of the Gα subunit is conserved despite poor conservation at the primary sequence level.



showing that *T. vaginalis* subunits TvG $\alpha$ 1 to TvG $\alpha$ 6 have conserved critical sites for myristoylation, phosphate, and Mg<sup>2+</sup> contact, as well as other residues critical for G $\alpha$  function. Note the degree of divergence between the G $\alpha$  subunits in the effector-contacting areas, the G $\beta\gamma$ -contact area, and the switch regions. Such high intra-organismal divergence at the sequence level has not been observed in any other organisms to date. m, myristoylation site; p, phosphate-contacting residues; W, tryptophan residues necessary for intrinsic fluorescence; g, guanine nucleotide-contacting residues; e, effector-contacting residues; m, magnesium-contacting residues;  $\beta$ , G $\beta$ -contacting residues; 4, key RGS-contacting residues; 6, a GTPase-deficient mutation (47). Note that *T. vaginalis* lacks genes encoding canonical G $\beta$  or G $\gamma$  subunits (Fig. 1A and fig. S1) (18). Consistent with the absence of these binding partners, *T. vaginalis* G $\alpha$  subunits lack critical residues in the G $\alpha$ -G $\beta\gamma$  binding interface, residues that are completely identical among human and land plant G $\alpha$  subunits. In other words, G $\alpha$  residues that form the G $\beta\gamma$ -binding surface were released from evolutionary constraint.

**Table S1.** Accession numbers of genes encoding G proteins, RGS proteins, and GPCRs.

	<i>G<math>\alpha</math></i>		<i>G<math>\beta</math></i>	<i>G<math>\gamma</math></i>	<i>RGS</i>	<i>cAMPR</i>	<i>GPCR</i>	<i>7TM-RGS</i>	<i>Data source and notes</i>	
<i>Trypanosoma brucei</i>	N/I		N/I	N/I	N/I	N/I	N/I	N/I	NCBI TriTrypDB( <a href="http://tritrypdb.org/">http://tritrypdb.org/</a> )	
<i>Leishmania major</i>	N/I		N/I	N/I	N/I	N/I	N/I	N/I	NCBI TriTrypDB( <a href="http://tritrypdb.org/">http://tritrypdb.org/</a> )	
<i>Giardia lamblia</i>	N/I		N/I	N/I	N/I	N/I	N/I	N/I	NCBI GiardiaDB( <a href="http://giardiadb.org/">http://giardiadb.org/</a> )	
<i>Trichomonas vaginalis</i>	XP_001322334.1 XP_001330268.1 XP_001580284.1 XP_001304281.1	XP_001325781.1 XP_001324344.1 XP_001316721.1	N/I	N/I	XP_001311154.1 XP_001583271.1 XP_001326285.1 XP_001320387.1	N/I	N/I	XP_001583271 XP_001326285 XP_001320387	NCBI TrichDB( <a href="http://trichdb.org/">http://trichdb.org/</a> )	
<i>Naegleria gruberi</i>	See ref. [18]		See ref. [18]	See ref. [18]	See ref. [18]	XP_002672980.1	N/I	N/I	NCBI, and see reference [18]	
<i>Arabidopsis thaliana</i>	AT2G26300.1 AT2G32460.1 AT4G34390.1	AT4G34390.1 AT1G31930.1	AT4G34460.1	AT3G3420.1 AT3G22942.1 AT5G20535.1	AT3G26090.1	NP_175261.1	N/I	AT3G26090.1	NCBI TAIR release 10	
<i>Selaginella moellendorffii</i>	XM_002960950.1 XP_002993179.1	XP_002970591.1	XP_002964323.1	See ref. [6]	XM_002984541.1	XP_002994399.1	N/I	XM_002984541.1	NCBI Phytozome v8.0( <a href="http://www.phytozome.net/">http://www.phytozome.net/</a> )	
<i>Physcomitrella patens</i>	XP_00172174.1		XP_001753169.1	See ref. [6]	N/I	XP_001784721.1 XP_001765654.1 XP_003060404.1	N/I	N/I	NCBI Phytozome v8.0( <a href="http://www.phytozome.net/">http://www.phytozome.net/</a> )	
<i>Micromonas pusilla</i>	N/I		N/I	N/I	N/I	N/I	N/I	N/I	NCBI JGI v2.0	
<i>Cyandioschyzon merolae</i>	N/I		N/I	N/I	N/I	N/I	N/I	N/I	Cyandioschyzon merolae genome project ( <a href="http://merolae.biol.s.u-tokyo.ac.jp/">http://merolae.biol.s.u-tokyo.ac.jp/</a> )	
<i>Cyanophora paradoxa</i>	N/I		N/I	N/I	N/I	N/I	N/I	N/I	Cyanophora genome project ( <a href="http://cyanophora.rutgers.edu/cyanophora/">http://cyanophora.rutgers.edu/cyanophora/</a> )	
<i>Guillardia theta</i>	N/I		N/I	N/I	N/I	N/I	N/I	N/I	JGI v1.0	
<i>Emiliania huxleyi</i>	431895 71535 442062	366493 43354	446896	N/I	452572 428179 466622	N/I	N/I	N/I	JGI v1.0	
<i>Thalassiosira pseudonana</i>	EED90460.1 EED88012.1		EED89370.1	FC517721.1*	XP_002288270.1 XP_002293773.1	N/I	XP_002291918.1 XP_002292162.1	N/I	NCBI, JGI v3.0 * NCBI EST database	
<i>Phaeodactylum tricoratum</i>	AC165128.1		EEC46675.1	N/I	N/I	N/I	XP_002184039.1 XP_002176439.1 XP_002176374.1 XP_002186461.1 XP_002181352.1 XP_002179604.1 XP_002181807.1	N/I	JGI v2.0 JGI Project ID: 3634397	
<i>Aureococcus anophagefferens</i>	EGB05471.1 EGB04190.1 EGB10363.1 EGB12735.1		EGB03726.1	N/I	EGB11309.1 EGB05279.1 EGB03131.1 EGB13909.1 EGB07294.1	EGB09262.1 EGB08936.1 EGB08116.1	EGB12570.1	N/I	JGI v1.0	
<i>Ectocarpus siliculosus</i>	CBJ30272.1 CBN74608.1 CBN79972.1 CBN76611.1 CBN73927.1 CBN75194.1		CBJ48797.1	FP268066.1*	CBN77641.1 CBN79604.1 CBN76971.1 CBN80153.1 CBN78214.1 CBJ32950.1 CBJ27735.1 CBJ27308.1 CBJ26968.1 CBJ33536.1 CBJ33442.1 CBJ33944.1 CBJ33186.1 CBJ33075.1 CBJ29641.1 CBJ32516.1 CBJ31998.1 CBJ25532.1 CBN77644.1 CBN78337.1 CBN77107.1 CBN80200.1 CBN73963.1 CBJ33441.1 CBJ33439.1 CBJ33076.1	CBJ33074.1 CBJ32612.1 CBJ26581.1 CBJ32515.1 CBJ32274.1 CBJ31531.1 CBJ31529.1 CBJ31527.1 CBJ31523.1 CBJ31489.1 CBJ31487.1 CBJ31485.1 CBJ26132.1 CBJ29972.1 CBJ31534.1 CBJ31526.1 CBJ31524.1 CBJ31522.1 CBJ31488.1 CBJ31486.1 CBJ30276.1 CBJ30154.1 CBJ28890.1 CBJ28886.1 CBJ28884.1	CBN74463.1	CBJ28378.1	CBJ31523.1 CBJ32274.1 CBN73963.1 CBJ31487.1 CBJ31485.1 CBJ33442.1 CBJ27735.1	NCBI * NCBI EST database
<i>Toxoplasma gondii</i>	N/I		N/I	N/I	N/I	N/I	N/I	N/I	NCBI	
<i>Paramecium tetraurelia</i>	N/I		N/I	N/I	N/I	NP_001448660.1 NP_001445405.1	NP_001446787.1 NP_001428100.1	N/I	NCBI	

<i>Tetrahymena thermophila</i>	N/I		N/I	N/I	N/I		XP_001457455.1 EAB89547.1 EAS00987.1 EAB89810.1	N/I	N/I	NCBI
<i>Bigeloviella natans</i>	20958 36381 36537 43366 43485 44744 45682 46389 48529 49183 49209 50213 51293 51362 52232 52805 54056 56289	56365 56705 56721 60790 62575 67038 73468 73904 79189 86504 87904 90090 90286 90299 90824 143654 147074	79237 54371 50917 92833 92207	N/I	63858 67758 68522 68565 71285 74263 75592 78234 78944 78991 80145 82144 84155	86284 87960 88269 90138 90636 90777 125472 127990 128479 133381 135776 144716 146368	81724 90233 84881 88731 144979 145130	79274 146547 138713 84266 85275 77411 90697 138747 130136 75367 75589	87960 128479 84059	JGI v1.0
<i>Dictyostelium discoideum</i>	EAL65751.1 EAL69280.1 EAL63880.1 EAL64550.1 EAL64268.1 EAL65814.1 EAL69181.1	EAL65161.1 EAL65694.1 EAL72990.1 EAL69252.1 EAL67402.1 EAL69377.1	EAL68757.1	EAL69955.1	EAL71154.1 EAL70454.1 EAL73296.1 EAL72779.1 EAL68050.1 EAL67970.1	EAL86151.1 EAL64415.1 EAL64379.1 EAL64164.1 EAL61591.1	See ref. [45]	See ref. [45]	N/I	NCBI Dictybase ( <a href="http://dictybase.org/">http://dictybase.org/</a> )
<i>Entamoeba histolytica</i>	EAL46350.2		EAL47361.2	Footnote 1	EAL50393.1 EAL47674.1	EAL42909.1	N/I	N/I	N/I	NCBI AmoebaDB ( <a href="http://amoebadb.org/">http://amoebadb.org/</a> )
<i>Saccharomyces cerevisiae</i>	AAA34650.1 AAB64553.1		CAA63175.1	DAA08871.1	NP_014750.3 NP_014945.3	NP_013557.1 NP_013603.1	N/I	NP_116627.2 NP_019743.1 NP_010249.1	N/I	NCBI See ref. [43] for RGS genes
<i>Neurospora crassa</i>	EAA27897.1 AAA02559.1 EAA32969.1 EAA31421.2		EAA27468.2	XP_956152.2	XP_957576.2 XP_963258.2 XP_962532.2	XP_958650.2 XP_965246.1 XP_958155.1	EAA35706.1 EAA28751.1 EAA28708.1	EAA3570.2 EAA35706.1 EAA33338.1 EAA28751.1 EAA28708.1	XP_958650.2	NCBI See ref. [44] for Gα, Gβ and GPCRs
<i>Capsaspora owczarzaki</i>	EFW45389.1 EFW45256.1 EFW40614.1 EFW47508.1	EFW41735.1 EFW46709.1 EFW39642.1 EFW44059.1	EFW39957.1 EFW44967.1	EFW42993.1	EFW47294.1 EFW47106.1 EFW46994.1 EFW46160.1 EFW45966.1 EFW45184.1 EFW44232.1 EFW43448.1	EFW41776.1 EFW40488.1 EFW40364.1 EFW44549.1 EFW43763.1 EFW41565.1 EFW41111.1 EFW40839.1	N/I	See ref. [17]	EFW44549.1 EFW41111.1 EFW46160.1	NCBI
<i>Trichoplax adhaerens</i>	EDV21414.1 EDV21413.1 EDV21511.1 EDV21241.1	EDV25537.1 EDV27798.1 EDV29483.1 EDV27799.1	EDV24201.1 EDV29817.1	EDV27301.1	XP_002118052.1 XP_002114968.1 XP_002114628.1 XP_002114610.1 XP_002114139.1 XP_002112504.1 XP_002110221.1	XP_002109778.1 XP_002109195.1 XP_002109868.1 XP_002109716.1 XP_002117882.1 XP_002115169.1 XP_002114043.1	See ref. [17, 31]	See ref. [17, 31]	N/I	NCBI